J Mol Neurosci (2008) 34:51–61
DOI 10.1007/s12031-007-0029-0

Diffusion Tensor Imaging (DTI)-based White Matter Mapping in Brain Research: A Review

Yaniv Assaf · Ofer Pasternak

Published online: 27 September 2007

Abstract Diffusion tensor imaging (DTI) has become one of the most popular MRI techniques in brain research, as well as in clinical practice. The number of brain studies with DTI is growing steadily and, over the last decade, has produced more than 700 publications. Diffusion tensor imaging enables visualization and characterization of white matter fascicli in two and three dimensions. Since the introduction of this methodology in 1994, it has been used to study the white matter architecture and integrity of the normal and diseased brains (multiple sclerosis, stroke, aging, dementia, schizophrenia, etc.). Although it provided image contrast that was not available with routine MR techniques, unique information on white matter and 3D visualization of neuronal pathways, many questions were raised regarding the origin of the DTI signal. Diffusion tensor imaging is constantly validated, challenged, and developed in terms of acquisition scheme, image processing, analysis, and interpretation. While DTI offers a powerful tool to study and visualize white matter, it suffers from inherent artifacts and limitations. The partial volume effect and the inability of the model to cope with non-Gaussian diffusion are its two main drawbacks. Nevertheless, when combined with functional brain mapping, DTI provides an efficient tool for comprehensive, noninvasive, functional anatomy mapping of the human brain. This review summarizes the development of DTI in the last decade with respect to the specificity and utility of the technique in radiology and anatomy studies.

Keywords Magnetic resonance imaging · White matter · Diffusion tensor imaging · Tractography · Anisotropy

Y. Assaf (✉)
Department of Neurobiochemistry, Faculty of Life Sciences,
Tel Aviv University, Tel Aviv 69978, Israel
e-mail: assafyan@post.tau.ac.il

Y. Assaf
Functional Brain Imaging Unit,
Tel Aviv Sourasky Medical Center, Tel Aviv 64239, Israel

O. Pasternak
Department of Computer Science, Faulty of Exact Sciences,
Tel Aviv University, Tel Aviv 69978, Israel

Background

Diffusion tensor imaging (DTI) revolutionalized the field of white matter mapping. This MRI-based methodology, originally presented in 1994 (Basser et al. 1994), takes advantage of the macroscopic geometrical arrangement of white matter bundles that becomes apparent through diffusion MRI measurements (Basser et al. 1994; Basser 1995; Basser and Jones 2002; Basser and Pierpaoli 1996, 1998; Pierpaoli et al. 1996; Pierpaoli and Basser 1996). In general, diffusion MRI measures the translational displacement of water molecules (Le Bihan 1995). The anisotropic nature of water displacement in white matter has been observed since the early days of diffusion MRI (Moseley et al. 1990, 1991; Sakuma et al. 1991), but its quantification, especially in the brain, was complicated. Water molecules' motion or diffusion was found to be much faster along the white matter fibers than perpendicular to them (Basser et al. 1994; Basser 1995; Basser and Pierpaoli 1996, 1998). The difference between these two motions (parallel and perpendicular to the fibers, also termed diffusion anisotropy) is the basis of DTI. Diffusion tensor imaging provides a framework for acquisition, analysis, and quantification of the diffusion properties of white matter (Basser and Pierpaoli 1996, 1998; Pierpaoli et al. 1996).

It takes diffusion measurements in multiple directions and, using tensor decomposition, extracts the diffusivities parallel and perpendicular to the fibers (also termed principal diffusivities, $\lambda_{//}$ and $\lambda_{\perp}$) (Basser et al. 1994; Basser 1995; Basser and Jones 2002; Basser and Pierpaoli 1996, 1998; Pierpaoli et al. 1996). These diffusivities are used for calculation of summation indices, such as the trace apparent diffusion coefficient (trADC, the mean of the diffusivities) or the fractional anisotropy (FA, the normalized standard deviation of the diffusivities) (Basser and Pierpaoli 1996, 1998; Pierpaoli et al. 1996; Pierpaoli and Basser 1996).

Dozens of diffusivity-based measures have been proposed (Pierpaoli and Basser 1996; Papadakis et al. 1999; Ulug and van Zijl 1999; Westin et al. 2002), but FA became the most widely used DTI-based index in brain research. Fractional anisotropy provides a gray-scale, 2D map, enhancing diffusion anisotropy differences with intensity limits between zero and one. In white matter, the anisotropy is high (approaching unity in most ordered areas), reflecting fast diffusivity along the fibers and slow diffusivity perpendicular to them (Pierpaoli et al. 1996); in gray matter and CSF, the anisotropy approaches zero as the diffusivity is similar in all directions. However, there is more to DTI than anisotropy measures. One of the major advantages of DTI is that it is rotationally invariant: it can measure the principal diffusivities regardless of the position of the fibers in space. Thus, one can extract not only the magnitude of the diffusivities but also their 3D alignment. In 1999, Pajevic and Pierpaoli suggested color-coded schemes to visualize this 3D information in two dimensions (Pajevic and Pierpaoli 1999). The most basic red–green–blue (RGB) color-coded scheme attributes a color for each orientation of the fibers: fibers crossing from left to right are visualized in red, fibers crossing anteriorly–posteriorly are visualized in green, and fibers crossing inferiorly–superiorly are

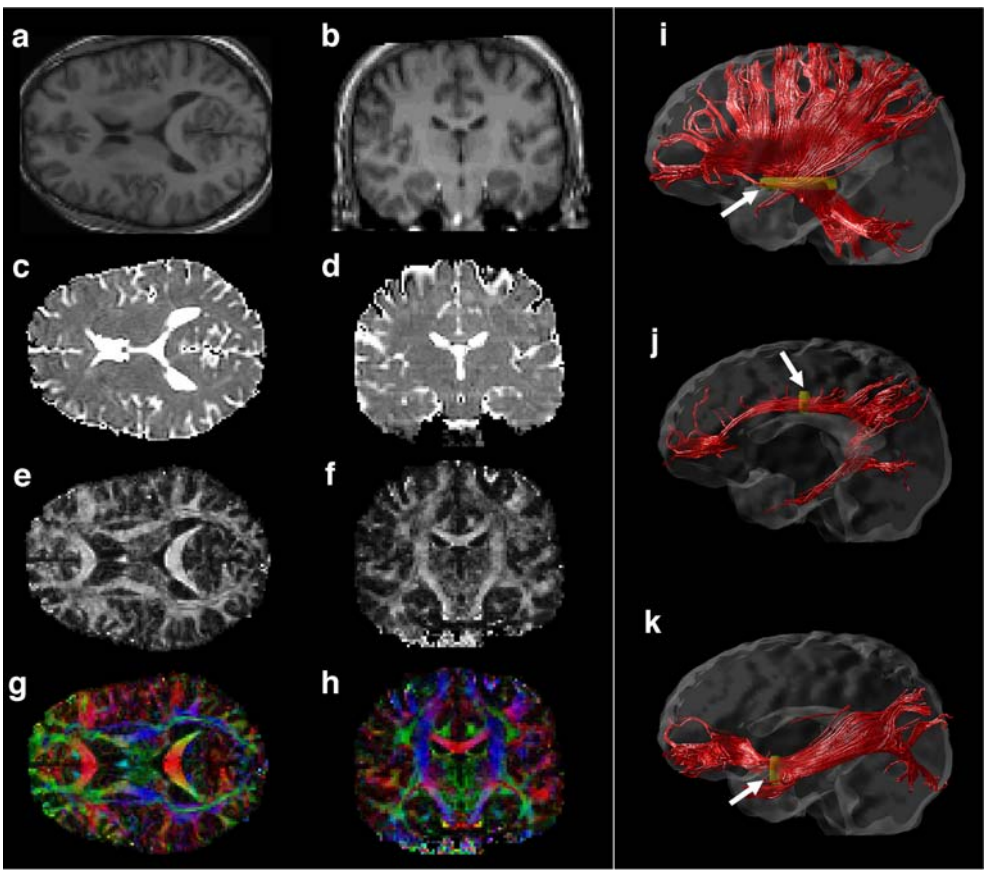

Figure 1 Diffusion tensor based images. **a** and **b** show axial (horizontal) and coronal T_1 weighted anatomical images. **c** and **d** trace ADC maps (mean diffusivity) of the same slices showed in **a** and **b**. **e**, **f** Fractional anisotropy maps showing high contrast between gray and white matter. **g**, **h** Color-coded FA maps depicting different fiber systems. With the presented color-coding, *red* represents fibers crossing from left to right, *green* crossing in the posterior anterior direction, and *blue* crossing in the inferior–superior direction in normal head coordinate system. **i**–**k** Three-dimensional tractography images of the same subject in **a**–**h**. **i** shows the corona radiata, **j** shows the cingulum, and **k** shows the inferior longitudinal fasciculus fiber systems. The *yellow* structures in **i**–**k** represent the seed ROI from which fibers were launched. All images were acquired at a resolution of 1.7×1.7×1.7 mm^3 at a 3T scanner with cardiac gated diffusion weighted echo planar imaging (*DW-EPI*, TE=105, b=1,000 s/mm^2 and 19 gradient directions)

visualized in blue (Pajevic and Pierpaoli 1999). Other color-coded schemes have been suggested since, but the most widely used is the simple RGB scheme.

Around the year 2000, groups used the 3D information embedded in DTI analysis to produce 3D virtual trajectories of white matter bundles (Basser et al. 2000; Conturo et al. 1999; Mori et al. 1999; Catani et al. 2002). These methodologies are intended to produce a continuous line based on the largest principal diffusivity, on the assumption that the largest diffusivity represents the motion along the fibers and its direction points to the geometrical 3D position of the fibers in each pixel. Techniques have been suggested for connecting the largest principal diffusivity vector field into trajectories (partial list: Basser et al. 2000; Conturo et al. 1999; Mori et al. 1999; Catani et al. 2002; Poupon et al. 2000) and were used to reconstruct a number of large fiber bundles (e.g., the pyramidal tract, corpus callosum, and superior longitudinal fascicules) (Mori et al. 1999; Catani et al. 2002).

Figure 1 summarizes the different levels of DTI analysis (trADC, FA, color-coded FA, and 3D fiber tractography) extracted from the same data set. While trADC maps show a similar averaged diffusivity across gray and white matters, FA significantly increases the specificity of the image for white matter. The color-coded FA maps and the 3D tractography images show the power of DTI to outline white matter architecture and fine structure usually hidden from conventional MRI. Using these different levels of DTI analysis, dozens of studies (currently producing more than 700 publications) have been performed to date, aimed at revealing the diffusion properties and architecture of the healthy brain and documenting DTI's clinical utility in various brain diseases and disorders. Besides determining the role of white matter integrity in various pathological conditions, DTI is now being used to study healthy brain connectivity. This review summarizes the contribution of DTI to the study of the pathophysiology of the brain, its contribution to radiological assessment and patient management, and its usefulness as a tool in neuroscience. The limits of DTI, the questions it can and cannot answer, and where it fails are emphasized.

DTI as a Physiological Tool (or What Do We Measure?)

Diffusion tensor imaging measures the displacement of water molecules on the micron scale and yields information about white matter fibers that pass within a pixel. The FA index is the most widely used parameter of DTI for representing the motional anisotropy of water molecules, being sensitive to the presence and integrity of white matter fibers. This white matter consists of thousands of neuronal fibers (axons) in each image pixel, as well as a dense array of various kinds of glial cells with oligodendrocytes that are unique to white matter. Oligodendrocytes make up the myelin sheaths that envelop the axons and ensure fast and efficient transmission of electrical signals through them. The question is to which cellular component the DTI signal is most sensitive. Do changes in the cellular arrangement around the axons change the motional anisotropy? Is myelin a crucial factor for obtaining motional anisotropy? The answers to these questions remain largely unknown, but since the diffusion MRI signal measured in DTI averages contributions from all compartments, it can be assumed that they all contribute to the observed anisotropy. Indeed, experimental observations in various pathological conditions support this assumption. We describe here the findings of DTI in three pathological conditions – demyelination, edema, and inflammation – that will help clarify the origins of the DTI signal.

Myelin is unique to white matter and is therefore believed to be one of the main effectors of the DTI signal. However, Beaulieu and Allen showed in 1994 that anisotropy in myelinated nerves and nonmyelinated nerves are similar. While it was true that myelin is not a prerequisite for obtaining diffusion anisotropy in neuronal tissue (Beaulieu and Allen 1994), subsequent experiments showed that anisotropy measures do indeed change significantly when myelin is damaged or absent (either in a demyelinating disease such as multiple sclerosis or in a premyelination condition at different stages of neuronal development) (Horsfield et al. 1998; Werring et al. 1999; Mukherjee et al. 2001; Huppi et al. 1998). In all these diseases and conditions, the absence of myelin paralleled reduced diffusion anisotropy. The exact contribution of myelin to the DTI signal and anisotropy measures is hard to estimate because other factors in demyelinating diseases and premyelination conditions may contribute to the observed signal (e.g., large volume of free diffusing water). Directly comparing two nerve types, one myelinated and the other nonmyelinated, as performed by Beaulieu and Allen (1994), is also limited because these tissues differ in many other factors such as axon diameter, extracellular matrix volume, and composition. Although the exact contribution of myelin to DTI could not be determined, it is reasonable to assume that it plays only a partial role. Indeed, FA measures in multiple sclerosis-diseased brains reveal significant anisotropy reduction in areas of lesions (see Fig. 2) (which may be attributed to increased water content, see below), but less dramatic effects in areas of normal-appearing white matter (NAWM) where demyelination is known to occur (Horsfield et al. 1998; Werring et al. 1999; Bammer et al. 2000; Assaf et al. 2002; Filippi et al. 2001; Ciccarelli et al. 2001). In addition, when DTI was used to characterize different lesion types (enhancing/nonenhancing) and different types of multiple sclerosis (primary progressive/relapsing remitting), the groups differed in diffusion

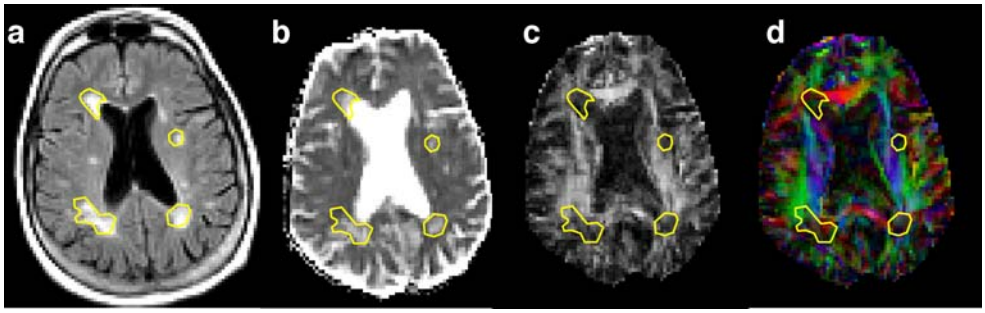

Figure 2 Diffusion tensor imaging of multiple sclerosis diseased patient. **a** FLAIR anatomical images showing few periventricular lesions (hyperintense spots marked by yellow frame). **b** trace ADC maps of the same slice shown in **a**. The mean diffusivity in the lesion is increased compared to the NAWM (see hyperintensity in the lesions). **c** Fractional anisotropy map of the same patient shows significantly reduced anisotropy within the lesions. **d** Color-coded FA maps showing the same observation as in **c**

anisotropy (Griffin et al. 2001; Filippi et al. 2001; Ciccarelli et al. 2001; Werring et al. 1999; Bammer et al. 2000).

Elevation in water content (edema) of a tissue changes the diffusion anisotropy. Edema does not necessarily affect the myelin or the axon itself, but it does change the weighted contribution of the cellular components in a pixel. Edema can be categorized into cellular edema, cytotoxic edema, as happens immediately following ischemia, and vasogenic edema, a typical reaction to inflammation (Ito et al. 1979; Betz et al. 1989). In cytotoxic edema, the intracellular volume (in white matter: glial cells) increases at the expense of the extracellular space and axons, whose cell bodies are most probably far from the site of infarction. This might lead to a reduction in axonal density. The DTI findings in cytotoxic edema are not uniform. Several DTI studies of acute stroke reported reduced anisotropy at the lesion site (Sorensen et al. 1999; Sotak 2002; Zelaya et al. 1999), while other studies reported increased anisotropy at the lesion site in some patients (Carano et al. 2000; Yang et al. 1999; Kafri et al. 2005). This contradictory behavior of DTI in cytotoxic edema remains to be evaluated (Green et al. 2002). In contrast, vasogenic edema (subacute stroke edema) is characterized only by marked reduction of FA values (Sotak 2002; Zelaya et al. 1999). A significant increase in extracellular volume most probably causes the reduction of axonal density per pixel and, hence, reduced anisotropy. Is it the reduction in axonal density (axonal loss) that leads to reduced anisotropy? Another explanation could be that axons within edema are loose and the geometrical arrangement of the tissue is less organized, leading to overall reduced anisotropy. On the other hand, it is likely to assume that some areas in the brain where fiber arrangement is denser do show increased anisotropy (e.g., corpus callosum). Again, we have here two distinct cellular processes that may lead to the same observation.

Leukoaraiosis refers to areas of nonspecific increased signal in T_2 weighted MRI. Leukoaraiosis is often found in the elderly population that suffers from hypertension or other vascular diseases (Kobari et al. 1990). Demyelinating disease such adrenoleukodystrophy (ALD) also display hyperintense areas on T_2 weighted MRI in widespread areas of white matter (Ito et al. 2001; Aubourg and Mandel 1996). The biochemical basis and pathological appearance of the two diseases differ, however: the main pathology in ALD is demyelination and affects mainly young children, while the origin of leukoaraiosis is largely unknown and probably represents vascular disease manifested by ischemic lesions affecting mainly the elderly. Both diseases show significant reduction in FA values in the areas of T_2 hyperintensity (Jones et al. 1999; Eichler et al. 2002), as well as diffusion changes in the NAWM. Similar FA changes are also observed in other pathologies characterized by T2 hyperintensity, such as tumor-related edema (Cruz and Sorensen 2005; Wick and Kuker 2004) and encephalopathy (Kealey and Provenzale 2002).

Changes in MRI signal can be attributed to a number of physiological factors including edema, demyelination, gliosis, and inflammation. Typically, FA will show a similar trend of reduction in all these pathologies and is therefore nonspecific. The fact that in DTI the observed signal is averaged over the entire pixel masks the ability to distinguish between the different pathologies affecting different cellular components. The vast majority of pathological processes in the brain will appear similar on FA maps. Perhaps the different processes can be teared apart by examining the different diffusivities and not their summation index, the FA.

DTI as a Radiological Tool (or What Is It Good For?)

Diffusion tensor imaging provides a new contrast mechanism. As noted above, FA maps exhibit a high signal in areas of significant anisotropic motion (as in white matter) and a low signal in areas of isotropic motion (as in gray matter and CSF). In the previous section, it was shown that

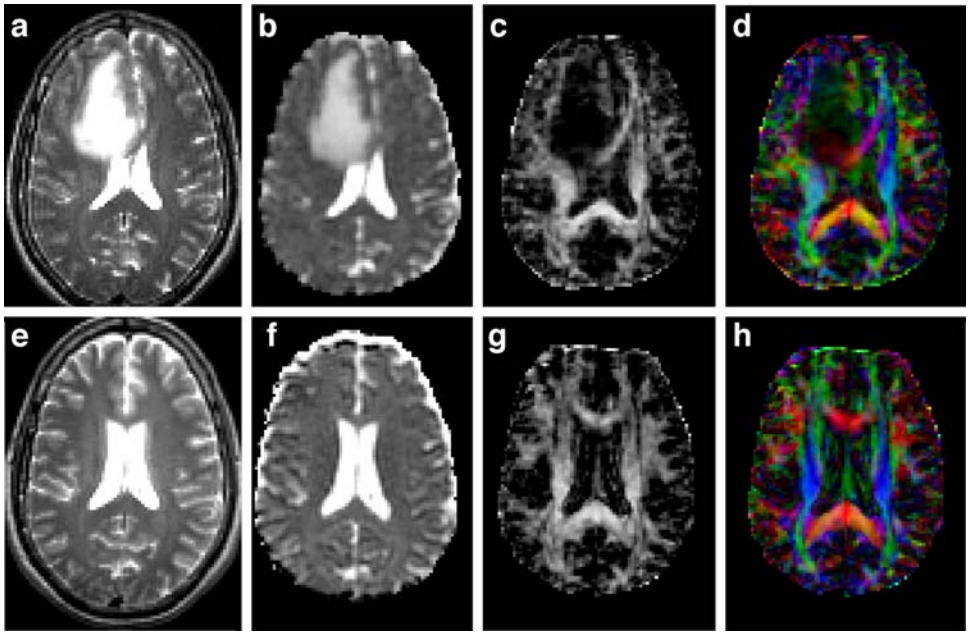

Figure 3 (**a**, T_2 weighted image) Brain-tumor-related edema (hyperintense area) characterized by increased diffusivity (**b**, trace ADC map) and reduced anisotropy (**c**, FA map). White matter of fiber directionality is not apparent within the edematous region (**c**, FA map, and **d**, color-coded FA map). After treatment, the edema was resolved (**e**, T_2 weighted image) and the trace ADC, FA, and color-coded FA shows normal appearance of the diffusion indices. In the acute phase of the edema, one could suspect that neuronal fibers might be damaged within the edematous region. However, the follow-up examination shows that the reduced anisotropy in the acute phase only represents in-direct effect of the edema and not the condition of the white matter fibers

FA changes are generally not specific and many factors can contribute to reduced anisotropy. In this section we ask what is the benefit of DTI from the standpoint of radiology?

Diffusion tensor imaging provides anatomical information with high specificity. In view of the ability of color-coded FA maps to distinguish between different fiber bundles based on their direction (see Fig. 1), it is not surprising that DTI is widely used today to delineate white matter around brain tumors (Witwer et al. 2002; Assaf et al. 2003; Clark et al. 2003; Sinha et al. 2002). Brain tumors can affect white matter fibers by either infiltrating or displacing the tissue. Studies have shown the utility of DTI in identifying the condition of white matter tracts within and surrounding the lesion using color-coded FA maps as well as tractography (Witwer et al. 2002; Assaf et al. 2003; Clark et al. 2003; Sinha et al. 2002). Figure 3 presents tumor-related brain lesions in two patients: in the first the tumor seems to displace the fibers, while in the other it seems to infiltrate them. These cases demonstrate the enormous impact of information provided by DTI on patient management and presurgical planning. A word of caution about the viability of the fibers: it is hard to

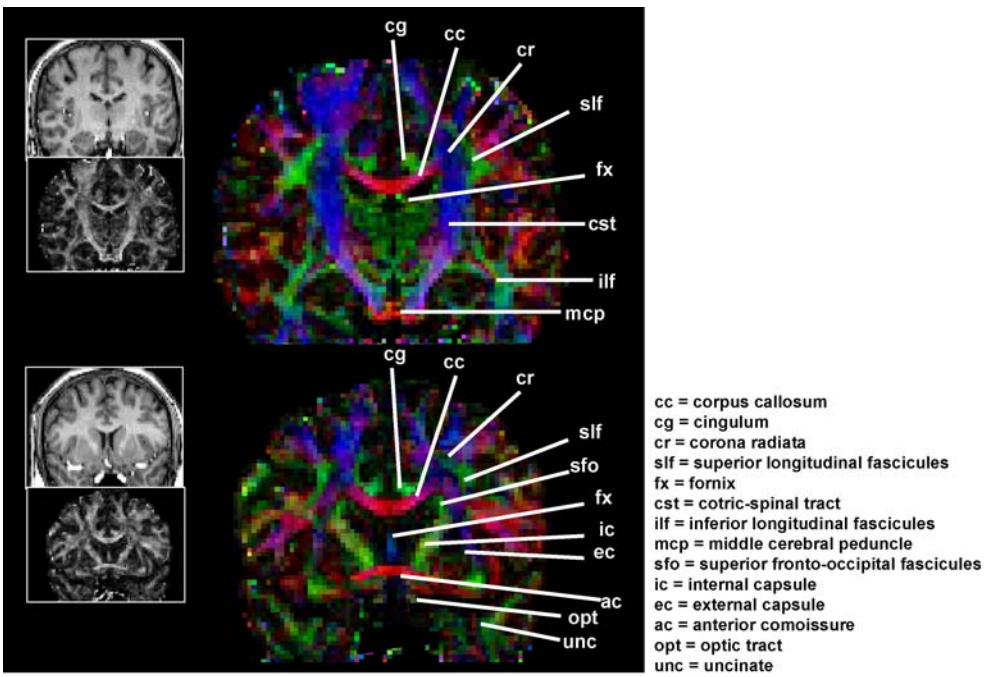

Figure 4 Coronal color-coded FA maps depicting a few fiber systems that can be identified (see *abbreviation* on the right). On the *top left* of each coronal slice are the T_1 and FA maps for comparison. It is possible to value the additional information embedded in the color-coded FA maps that help identifying the distinct fiber system. For more detailed information regarding which fiber systems can be viewed with DTI, please refer to Mori et al. (2005)

Table 1 Publications on FA changes in neurological disorders

AWM					NAWM				
Disease/lesion	FA			Reference	Disease/lesion	FA			Reference
	At lesion	Control	% change			At lesion	Control	% change	
MS (T_1 isointense)	0.43±0.22	N/A	−37	Bammer et al. 2000	MS (internal capsule)	0.63±0.06	0.68±0.07	−7	Bammer et al. 2000
MS (T_1 hyperintense)	0.32±0.09	N/A	−44	Bammer et al. 2000	MS (frontal white matter)	0.39±0.05	0.43±0.03	−9	Bammer et al. 2000
MS (Gd enhanced)	0.44±0.12	N/A	−22	Bammer et al. 2000	MS (corpus callosum)	0.75±0.06	0.79±0.05	−13	Bammer et al. 2000
MS (ring enhanced)	0.23±0.01	N/A	−38	Bammer et al. 2000	MS (centrum semiovale)	0.46±0.06	0.53±0.07	−5	Bammer et al. 2000
MS	0.39±0.11	0.54±0.15	−28	Assaf and Cohen 2002	MS	0.52±0.15	0.54±0.15	−4	Assaf and Cohen 2002
Stroke	0.29±0.11	0.48±0.15	−40	Werring et al. 2000	Stroke	0.39±0.04	0.45±0.04	−13	Thomalla et al. 2004
Leukoaraiosis	0.17±0.04	0.34±0.05	−48	Jones et al. 1999	Leukoaraiosis	0.29±0.05	0.34±0.05	−13	Jones et al. 1999
Leukoaraiosis	0.25±0.06	0.38±0.06	−35	Jones et al. 1999	Leukoaraiosis	0.35±0.06	0.38±0.06	−7	Jones et al. 1999
Leukoaraiosis	0.18±0.03	0.31±0.02	−41	Jones et al. 1999	Leukoaraiosis	0.30±0.03	0.31±0.02	−4	Jones et al. 1999
ALD	0.28±0.03	0.46±0.05	−39	Eichler et al. 2002	Aging (corpus callosum)	0.80±0.07	0.83±0.05	−4	Salat et al. 2005
Tumor (meningioma)	0.28±0.09	N/A	−37	Lu et al. 2004	Aging (internal capsule)	0.53±0.06	0.59±0.04	−10	Salat et al. 2005
Tumor (LGM)	0.25±0.04	N/A	−43	Lu et al. 2004	Aging (frontal WM)	0.30±0.03	0.42±0.04	−29	Salat et al. 2005
Tumor (GBM)	0.24±0.04	N/A	−45	Lu et al. 2004	Epilepsy	0.34±0.06	0.43±0.09	−21	Dumas de la Roque et al. 2005
Tumor (metastasa)	0.21±0.03	N/A	−52	Lu et al. 2004	AD	0.38±0.08	0.42±0.09	−10	Fellgiebel et al. 2004
					AD	0.62±0.11	0.69±0.09	−9	Fellgiebel et al. 2004
					AD (cingulum)	0.47±0.10	0.58±0.07	−19	Fellgiebel et al. 2005
					MCI	0.39±0.07	0.42±0.09	−7	Fellgiebel et al. 2004
					MCI	0.64±0.11	0.69±0.09	−7	Fellgiebel et al. 2004
					MCI (cingulum)	0.52±0.06	0.58±0.07	−10	Fellgiebel et al. 2004
					Schizophrenia	0.34±0.03	0.35±0.08	−3	Kumra et al. 2004
					Schizophrenia	0.34±0.04	0.38±0.05	−11	Kumra et al. 2004

AD = dementia of Alzheimer's type, MCI = mild cognitive impairment

estimate the pathological state of the tissue, especially in areas of tumor infiltration into the white matter where FA values are extremely low. Reduced FA might be related to disintegration of the fibers, but a significant increase in water content (edema) without any effect on the fibers themselves can give the same FA reading.

The radiological use of DTI in other neurological disorders is ambiguous. As described previously, FA has a tendency to be low in pathological conditions. Table 1 summarizes several publications on FA changes in a few neurological disorders. We divided the pathologies into those with signal changes in T_2 weighted MRI (abnormal white mater, AWM) and those in which the white matter appears normal by conventional imaging (NAWM). Fractional anisotropy changes for AWM are highly significant (−39±8%) and, therefore, visible to the radiologist's eye; FA changes in NAWM are more subtle (−11±7%) and cannot be identified, visibly or quantitatively, on a single subject in the typical FA images standard deviations (ranges from 10–20%). Although impressive FA changes were found in focal regions (e.g., frontal areas in aging and cingulum in dementia) for some of the disorders presented in Table 1, in most cases significant changes were found only when relatively large samples ($n>10$ subjects) were analyzed. Unsurprisingly, as important as such information is for research, it cannot be used for radiological assessment.

Psychiatric disorders are one field in which MRI-based radiology has not been able to identify specific patterns of brain abnormalities. In recent years the hypothesis of disconnection syndrome as a crucial contributor to psychiatric disorders has become increasingly popular, pointing to white matter involvement in such diseases (Catani and Ffytche 2005; Magaro and Page 1983). The most studied psychiatric disease is schizophrenia, where the major finding is reduced FA in widespread brain regions including the corpus callosum, uncinate fascicules, frontal white matter, and others (Kanaan et al. 2005; Kubicki et al. 2005; Jones et al. 2005; Kumra et al. 2004; Ardekani et al. 2003; Lim and Helpern 2002; Price et al. 2005). Other studies on psychiatric disorders and diseases include dementia of Alzheimer's type, mild cognitive impairment (Fellgiebel et al. 2004, 2005; Bozzali et al. 2002; Moseley et al. 2002; Medina et al. 2005), and obsessive compulsive disorder (Szeszko et al. 2005), all of which reported reduced FA in various brain regions. These studies indicate a role for white matter changes in psychiatric disorders but do not identify a specific pattern of brain changes for a particular disease. Moreover, the subtle changes that most likely occur in the white matter of psychiatric subjects could be detected only following group analysis. In a recent paper, Jones et al. (2005) raised the problem of voxel-based morphometry, which is a preferred approach for group comparisons; they concluded that the identification of subtle FA changes might be dependent on the analysis procedure (smoothing kernel) and may not be reporting real pathophysiological changes.

The radiological benefits of DTI seem to be limited. In the vast majority of diseases, AWM (typically defined so by T2 weighted MRI) is characterized also by reduced FA. In areas of NAWM, FA measurement reports significant changes not apparent on conventional MRI, but those changes are typically small and may be less apparent on a single subject level. One of DTI's major advantages is its ability to discriminate between different white matter structures, thus having great radiological value in diseases where fibers are distorted (as in brain tumors).

DTI as an Anatomical Tool (or To Track or Not To Track?)

Figure 4 shows color-coded FA maps in coronal sections of a healthy volunteer depicting distinct white matter structures that look as if they were taken from an anatomy textbook. Indeed, the information embedded in the color-coded FA maps, if produced at high spatial resolution, can show even small fiber systems (e.g., the anterior comissure). Such high-resolution data were the basis of a recent DTI-based white matter atlas identifying as many as 42 white matter systems (Mori et al. 2005).

Color-coded FA maps are only one way to show the directional information embedded in DTI. Three-dimensional tractography, proposed by researchers around the year 2000, reconstructs fiber systems based on DTI's eigenvector fields (Basser et al. 2000; Conturo et al. 1999; Mori et al. 1999; Catani et al. 2002). The possibility to track a fiber system pushed MRI to the field of anatomical connectivity—locating the trajectory of a distinct fiber system. Anatomical connectivity was previously limited to tracer histological methods, which obviously could not be applied on a human brain noninvasively. Tractography is prone to error, some subjective and some inherent in the DTI model, and since its advent, considerable effort has been devoted to validating its results.

The key step in DTI-based tractography is selecting a seed region of interest (ROI) from which virtual fibers will be launched. To select a specific fiber system, one has to know a priory the anatomy of white matter. For instance, to show the coritco-spinal tract, one would choose seed ROI at the level of the internal capsule where these fibers are known to pass. This might be a problem when dealing with smaller fiber systems where partial volume occurs and the identification of the location of the fiber system is difficult. To track such systems, defining the seed ROI requires numerous trial and error attempts. The identification of a fiber system becomes even more complicated for patients whose brain structure is distorted (e.g., by a lesion). A few

groups suggested using constrain on the tracking to help identify the start and end points of a track (usually by functional MRI) (Hendler et al. 2003; Parmar et al. 2004; Guye et al. 2003; Schonberg et al. 2005).

Seed ROI selection is only one of several problems inherent in the DTI model. The DTI model consists of two assumptions that are not necessarily true for brain white matter tissue. The first is that the diffusion in white matter is Gaussian (i.e., the displacement probability of water molecules is Gaussian) (Basser 1995). Compartmentalization and restricted diffusion certainly lead to non-Gaussian diffusion (Assaf and Cohen 2000; Beaulieu 2002; Assaf and Basser 2005; Alexander et al. 2002; Jensen et al. 2005). Experimental evidence points to non-Gaussian diffusion in white matter, although this becomes apparent only at nonconventional experimental conditions (*b* value> 2,500 s/mm^2) (Assaf and Cohen 2000; Beaulieu 2002; Assaf and Cohen 1998; Cohen and Assaf 2002). It should be noted that so far modeling the non-Gaussian diffusion in brain is ill-posed. The second assumption of DTI is that it is sufficient to use a single diffusion tensor to characterize each pixel. A typical pixel in DTI experiments with a volume of 2.5×2.5×2.5 mm^3 includes tens of thousands of axons and glial cells surrounded by extracellular matrix. It is unlikely that those compartments are represented by a single diffusion tensor. Thus, the measured diffusion tensor is an average of these compartments. Areas of tissue partial volume (where white/gray matter or white matter/CSF reside in the same pixel) or of white matter partial volume (where two fiber systems cross the same pixel often in different orientations) are examples of where the DTI model will fail (Papadakis et al. 2002; Tuch et al. 2002; Jansons and Alexander 2003). Indeed, areas of white matter where two or more fiber systems pass within the same pixel will appear hypointense; the DTI model cannot account for the two systems and will interpret them as low anisotropy.

The aforementioned problems are evident on the 2D FA maps depicted in Fig. 5. Measurement of FA values in such areas reduces the reliability of the observation, as it will not represent the real diffusion anisotropy. Moreover, tractography of the fiber system passing through such a region may result in premature ending of the virtual fiber or merging of two fiber systems into one bundle. A typical artifact of that kind is the fanning of the pyramidal tract into the primary motor and sensory cortices. When placing a seed ROI in the internal capsule, one expects the fiber to

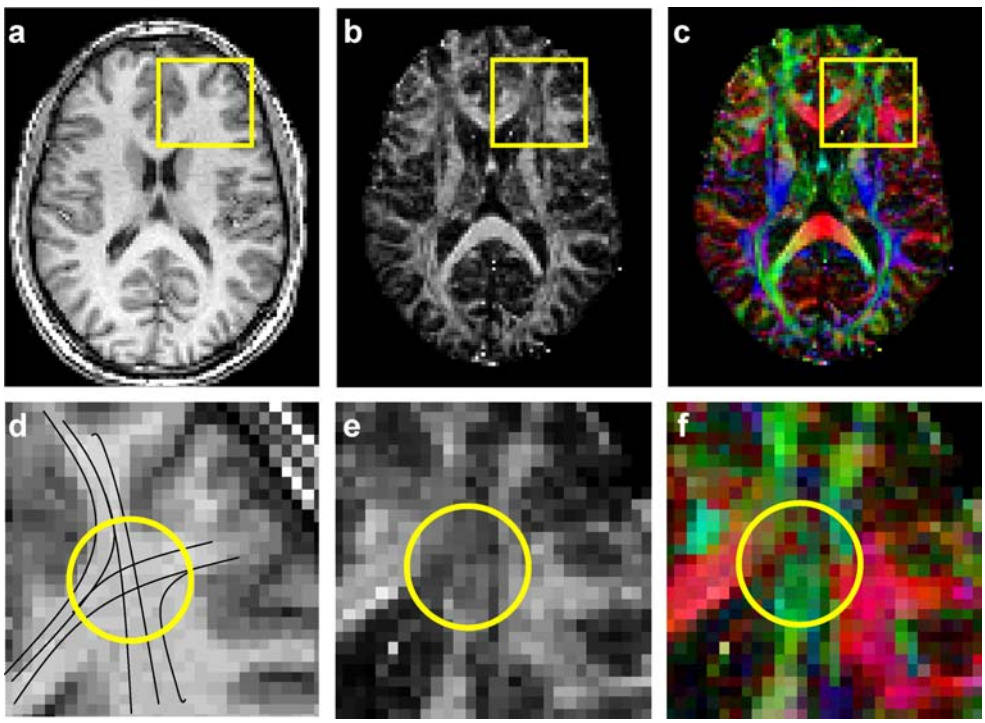

Figure 5 Example for partial volume artifact in DTI. **a** T_1 weighted anatomical image with the right frontal region enlarged at **d** including line drawings of the different fiber systems that pass in that region: one arriving from the genu of the corpus callusm and the other from the thalamic radiation of the internal capsule, both projecting into the frontal lobe. **b** shows the FA maps enlarged at **e**, showing a low anisotropy area (marked by *yellow circle*) in the area of crossing fiber systems. This is also showing in the color-coded FA maps (**c** and **f**) where one can follow the direction of the fiber (*red* for the corpus callosum and *green* for the thalamic radiation). In the crossing fiber region the observed color is a mix of the two fiber systems. Because two crossing fibers reside within the same pixel in that region, the diffusion is hindered in all measured directions, which artifactually can be characterized by isotropic diffusion and, thus, reduced FA

fan into their cortical origin. However, most fibers tend to end prematurely at the ventricles level, or to reach only the leg-related motor cortical area. This happens because other fiber systems cross at the level of the ventricles, significantly reducing the anisotropy and changing the eigen vector to an average between the two systems. Groups have suggested several analytic and experimental frameworks to deal with this problem (Tuch et al. 2002; Tuch 2004; Jansons and Alexander 2003; Pasternak et al. 2004). The most straightforward method is the multiple tensor (MT) one (Tuch et al. 2002), in which more than one tensor is allowed to reside in each pixel; however, the certainty in estimating these two tensors is low (Assaf and Basser 2005). Other methods try to enhance the MT by adding additional constrains (MTV), or acquiring the diffusivity at high angular resolution and allowing the visualization of multiple fiber orientations (Jansons and Alexander 2003; Pasternak et al. 2004, 2006). These methodologies are still being developed and none are used routinely to overcome the partial volume effect. Moreover, inherently, all the above assume that diffusion is Gaussian and therefore do not account for the first false assumption of DTI.

The Future of DTI

Diffusion tensor imaging is a powerful tool for the visualization of white matter structures. The growing number of DTI-based studies, applied and methodological, shows the great potential of the method. The fact that DTI assumes Gaussian diffusion limits its applications. It averages information from different compartments and reduces the certainty of tracking in partial-value pixels. The problem of non-Gaussian diffusion has been studied and solved theoretically for defined nonbiologically related structures (e.g., porous material) in the so-called "q-space" framework (Callaghan 1991; Callaghan et al. 1991). Cory and Garroway (1990) used this approach on yeast cells and showed that one can take advantage of non-Gaussian diffusion to extract geometrical features on the samples (Cory and Garroway 1990). In the late 1990s, this approach was implemented on white matter, and the terms q-space imaging and diffusion spectrum imaging of the human brain were coined (Assaf and Cohen 2000; Assaf et al. 2002; Tuch et al. 2003), and later on, the CHARMED model was formed (Assaf et al. 2005). Although these methodologies provide a better theoretical basis on which to address the complicated diffusion of water in white matter, experimentally, they are time consuming and require strong computation power. They cannot replace the fast acquisition and analysis of DTI, but most certainly can yield additional, complementary information that is hidden from DTI.

References

Alexander, D. C., Barker, G. J., & Arridge, S. R. (2002). Detection and modeling of non-Gaussian apparent diffusion coefficient profiles in human brain data. *Magnetic Resonance in Medicine, 48*, 331–340.

Ardekani, B. A., Nierenberg, J., Hoptman, M. J., Javitt, D. C., & Lim, K. O. (2003). MRI study of white matter diffusion anisotropy in schizophrenia. *NeuroReport, 14*, 2025–2029.

Assaf, Y., & Basser, P. J. (2005). Composite hindered and restricted model of diffusion (CHARMED) MR imaging of the human brain. *NeuroImage, 27*, 48–58.

Assaf, Y., & Cohen, Y. (1998). Non-mono-exponential attenuation of water and N-acetyl aspartate signals due to diffusion in brain tissue. *Journal of Magnetic Resonance, 131*, 69–85.

Assaf, Y., & Cohen, Y. (2000). Assignment of the water slow-diffusing component in the central nervous system using q-space diffusion MRS: implications for fiber tract imaging. *Magnetic Resonance in Medicine, 43*, 191–199.

Assaf, Y., Ben-Bashat, D., Chapman, J., Peled, S., Biton, I. E., Kafri, M., et al. (2002). High b-value q-space analyzed diffusion-weighted MRI: application to multiple sclerosis. *Magnetic Resonance in Medicine, 47*, 115–126.

Assaf, Y., Pianka, P., Rothstein, P., Sigal, M., & Hendler, T. (2003). Deviation of fiber tracts in the vicinity of brain lesions: evaluation by diffusion tensor imaging. *Israel Journal of Chemistry, 43*, 155–163.

Aubourg, P., & Mandel, J. L. (1996). X-linked adrenoleukodystrophy. *Annals of the New York Academy of Sciences, 804*, 461–476.

Beaulieu, C. (2002). The basis of anisotropic water diffusion in the nervous system—a technical review. *NMR in Biomedicine, 15*, 435–455.

Bammer, R., Augustin, M., Strasser-Fuchs, S., Seifert, T., Kapeller, P., Stollberger, R., et al. (2000). Magnetic resonance diffusion tensor imaging for characterizing diffuse and focal white matter abnormalities in multiple sclerosis. *Magnetic Resonance in Medicine, 44*, 583–591.

Basser, P. J. (1995). Inferring microstructural features and the physiological state of tissues from diffusion-weighted images. *NMR in Biomedicine, 7–8*, 333–344.

Basser, P. J., & Jones, D. K. (2002). Diffusion-tensor MRI: theory, experimental design and data analysis—a technical review. *NMR in Biomedicine, 15*, 456–467.

Basser, P. J., & Pierpaoli, C. (1996). Microstructural and physiological features of tissues elucidated by quantitative-diffusion-tensor MRI. *Journal of Magnetic Resonance Series B, 111*, 209–219.

Basser, P. J., & Pierpaoli, C. (1998). A simplified method to measure the diffusion tensor from seven MR images. *Magnetic Resonance in Medicine, 39*, 928–934.

Basser, P. J., Mattiello, J., & Le Bihan, D. (1994). MR diffusion tensor spectroscopy and imaging. *Biophysical Journal, 66*, 259–267.

Basser, P. J., Pajevic, S., Pierpaoli, C., Duda, J., & Aldroubi, A. (2000). In vivo fiber tractography using DT-MRI data. *Magnetic Resonance in Medicine, 44*, 625–632.

Beaulieu, C., & Allen, P. S. (1994). Determinants of anisotropic water diffusion in nerves. *Magnetic Resonance in Medicine, 31*, 394–400.

Betz, A. L., Iannotti, F., & Hoff, J. T. (1989). Brain edema: a classification based on blood–brain barrier integrity. *Cerebrovascular and Brain Metabolism Reviews, 11*, 133–154.

Bozzali, M., Falini, A., Franceschi, M., Cercignani, M., Zuffi, M., Scotti, G., et al. (2002). White matter damage in Alzheimer's disease assessed in vivo using diffusion tensor magnetic resonance imaging. *Journal of Neurology, Neurosurgery and Psychiatry, 72*, 742–746.

Callaghan, P. T. (Ed.) (1991). *Principles of Nuclear Magnetic Resonance Microscopy*. Oxford: Oxford University Press.

Callaghan, P. T., Coy, A., MacGowan, D., Packer, K. J., & Zelaya, F. O. (1991). Diffraction like effects in NMR diffusion studies of fluid in porous solids. *Nature, 351*, 467–469.

Carano, R. A., Li, F., Irie, K., Helmer, K. G., Silva, M. D., Fisher, M., et al. (2000) Multispectral analysis of the temporal evolution of cerebral ischemia in the rat brain. *Journal of Magnetic Resonance Imaging, 12*, 842–858.

Catani, M., & Ffytche, D. H. (2005). The rises and falls of disconnection syndromes. *Brain, 128*, 2224–2239.

Catani, M., Howard, R. J., Pajevic, S., & Jones, D. K. (2002). Virtual in vivo interactive dissection of white matter fasciculi in the human brain. *NeuroImage, 17*, 77–94.

Ciccarelli, O., Werring, D. J., Wheeler-Kingshott, C. A., Barker, G. J., Parker, G. J., Thompson, A. J., et al. (2001). Investigation of MS normal-appearing brain using diffusion tensor MRI with clinical correlations. *Neurology, 56*, 926–933.

Clark, C. A., Barrick, T. R., Murphy, M. M., & Bell, B. A. (2003). White matter tracking in patients with space-occupying lesions of the brain: a new technique for neurosurgical planning? *NeuroImage, 20*, 1601–1608.

Cohen, Y., & Assaf, Y. (2002). High b-value q-space analyzed diffusion-weighted MRS and MRI in neuronal tissues—a technical review. *NMR in Biomedicine, 15*, 516–542.

Conturo, T. E., Lori, N. F., Cull, T. S., Akbudak, E., Snyder, A. Z., Shimony, J. S., et al. (1999). Tracking neuronal fiber pathways in the living human brain. *Proceedings of the National Academy of Sciences of the United States of America, 96*, 10422–10427.

Cory, D. G., & Garroway, A. N. (1990). Measurement of translational displacement probabilities by NMR—an indicator of compartmentation. *Magnetic Resonance in Medicine, 14*, 435–444.

Cruz, Jr, L. C., & Sorensen, A. G. (2005). Diffusion tensor magnetic resonance imaging of brain tumors. *Neurosurgery Clinics of North America, 16*, 115–134.

Dumas de la Roque, A., Oppenheim, C., Chassoux, F., Rodrigo, S., Beuvon, F., Daumas-Duport, C., et al. (2005). Diffusion tensor imaging of partial intractable epilepsy. *European Radiology, 15*, 279–285.

Eichler, F. S., Itoh, R., Barker, P. B., Mori, S., Garrett, E. S., van Zijl, P. C., et al. (2002). Proton MR spectroscopic and diffusion tensor brain MR imaging in X-linked adrenoleukodystrophy: initial experience. *Radiology, 225*, 245–252.

Fellgiebel, A., Muller, M. J., Wille, P., Dellani, P. R., Scheurich, A., Schmidt, L. G., et al. (2005). Color-coded diffusion-tensor-imaging of posterior cingulate fiber tracts in mild cognitive impairment. *Neurobiology of Aging, 26*, 1193–1198.

Fellgiebel, A., Wille, P., Muller, M. J., Winterer, G., Scheurich, A., Vucurevic, G., et al. (2004). Ultrastructural hippocampal and white matter alterations in mild cognitive impairment: a diffusion tensor imaging study. *Dementia and Geriatric Cognitive Disorders, 18*, 101–108.

Filippi, M., Cercignani, M., Inglese, M., Horsfield, M. A., & Comi, G. (2001). Diffusion tensor magnetic resonance imaging in multiple sclerosis. *Neurology, 56*, 304–311.

Green, H. A., Pena, A., Price, C. J., Warburton, E. A., Pickard, J. D., Carpenter, T. A., et al. (2002). Increased anisotropy in acute stroke: a possible explanation. *Stroke, 33*, 1517–1521.

Griffin, C. M., Chard, D. T., Ciccarelli, O., Kapoor, B., Barker, G. J., Thompson, A. I., et al. (2001). Diffusion tensor imaging in early relapsing-remitting multiple sclerosis. *Multiple Sclerosis, 7*, 290–297.

Guye, M., Parker, G. J., Symms, M., Boulby, P., Wheeler-Kingshott, C. A., Salek-Haddadi, A., et al. (2003). Combined functional MRI and tracotgraphy to demonstrate the connectivity of the human primary motor cortex in vivo. *NeuroImage, 19*, 1349–1360

Hendler, T., Pianka, P., Sigal, M., Kafri, M., Ben-Bashat, D., Constantini, S., et al. (2003). Delineating gray and white matter involvement in brain lesions: 3D alignment of fMRI and DTI. *Journal of Neurosurgery, 99*, 1018–1027.

Horsfield, M. A., Larsson, H. B., Jones, D. K., & Gass, A. (1998). Diffusion magnetic resonance imaging in multiple sclerosis. *Journal of Neurology, Neurosurgery and Psychiatry, 64*(S1), S80–S84.

Huppi, P. S., Maier, S. E., Peled, S., Zientara, G. P., Barnes, P. D., Jolesz, F. A., et al. (1998). Microstructural development of human newborn cerebral white matter assessed in vivo by diffusion tensor magnetic resonance imaging. *Pediatric Research, 44*, 584–590.

Ito, R., Melhem, E. R., Mori, S., Eichler, F. S., Raymond, G. V., & Moser, H. W. (2001). Diffusion tensor brain MR imaging in X-linked cerebral adrenoleukodystrophy. *Neurology, 56*, 544–547.

Ito, U., Ohno, K., Nakamura, R., Suganuma, F., & Inaba, Y. (1979). Brain edema during ischemia and after restoration of blood flow. Measurement of water, sodium, potassium content and plasma protein permeability. *Stroke, 10*, 542–547.

Jansons, K. M., & Alexander, D. C. (2003). Persistent angular structure: new insights from diffusion MRI data. Dummy version. *Information Processing in Medical Imaging, 18*, 672–683.

Jensen, J. H., Helpern, J. A., Ramani, A., Lu, H., & Kaczynski, K. (2005). Diffusional kurtosis imaging: the quantification of non-Gaussian water diffusion by means of magnetic resonance imaging. *Magnetic Resonance in Medicine, 53*, 1432–1440.

Jones, D. K., Lythgoe, D., Horsfield, M. A., Simmons, A., Williams, S. C., & Markus, H. S. (1999). Characterization of white matter damage in ischemic leukoaraiosis with diffusion tensor MRI. *Stroke, 30*, 393–397.

Jones, D. K., Symms, M. R., Cercignani, M., & Howard, R. J. (2005). The effect of filter size on VBM analyses of DT-MRI data. *NeuroImage, 26*, 546–554.

Kafri, M., Bova, I., Pianka, P., Aizenstein, O., Hendler, T., Borenstein, N., et al. (2005). Segmented ROI Analysis of DTI in Stroke. *Proceedings of the International Society for Magnetic Resonance in Medicine, 12*, 1373.

Kanaan, R. A., Kim, J. S., Kaufmann, W. E., Pearlson, G. D., Barker, G. J., & McGuire, P. K. (2005). Diffusion tensor imaging in schizophrenia. *Biological Psychiatry, 58*, 921–929.

Kealey, S. M., & Provenzale, J. M. (2002). Tensor diffusion imaging in B12 leukoencephalopathy. *Journal of Computer Assisted Tomography, 26*, 952–955.

Kobari, M., Meyer, J. S., Ichijo, M., & Oravez, W. T. (1990). Leukoaraiosis: correlation of MR and CT findings with blood flow, atrophy, and cognition. *American Journal of Neuroradiology, 11*, 273–281.

Kubicki, M., McCarley, R., Westin, C. F., Park, H. J., Maier, S., Kikinis, R., et al. (2005). A review of diffusion tensor imaging studies in schizophrenia. *Journal of Psychiatric Research, 41*, 15–30.

Kumra, S., Ashtari, M., McMeniman, M., Vogel, J., Augustin, R., Becker, D. E., et al. (2004) Reduced frontal white matter integrity in early-onset schizophrenia: a preliminary study. *Biological Psychology, 55*, 1138–1145.

Le Bihan, D. (Ed.) (1995). *Diffusion and Perfusion MRI, 1st Edition*. New York: Raven.

Lim, K. O., & Helpern, J. A. (2002). Neuropsychiatric applications of DTI—a review. *NMR in Biomedicine, 15*, 587–593.

Lu, S., Ahn, D., Johnson, G., Law, M., Zagzag, D., & Grossman, R. I. (2004). Diffusion-tensor MR imaging of intracranial neoplasia and associated peritumoral edema: introduction of the tumor infiltration index. *Radiology, 232*, 221–228.

Magaro, P. A., & Page, J. (1983). Brain disconnection, schizophrenia, and paranoia. *The Journal of Nervous and Mental Disease, 171*, 133–140.

Medina, D., Detoledo-Morrell, L., Urresta, F., Gabrieli, J. D., Moseley, M., Fleischman, D., et al. (2005) White matter changes in mild cognitive impairment and AD: A diffusion tensor imaging study. *Neurobiology of Aging, 27*, 663–672.

Mori, S., Crain, B. J., Chacko, V. P., & van Zijl, P. C. M. (1999). Three dimensional tracking of axonal projections in the brain by magnetic resonance imaging. *Annals of Neurology, 45*, 265–269.

Mori, S., Wakana, S., Nagae-Poetscher, L. M., & van Zijl, P. C. M. (Eds.) (2005). *MRI Atlas of Human White Matter, 1st Edition*. Amsterdam: Elsevier.

Moseley, M., Bammer, R., & Illes, J. (2002). Diffusion-tensor imaging of cognitive performance. *Brain and Cognition, 50*, 396–413.

Moseley, M. E., Cohen, Y., Kucharczyk, J., Mintorovitch, J., Asgari, H. S., Wendland, M. F., et al. (1990). Diffusion-weighted MR imaging of anisotropic water diffusion in cat central-nervous-system. *Radiology, 176*, 439–445.

Moseley, M. E., Hucharczyk, J., Asgari, H. S., & Norman, D. (1991). Anisotropy in diffusion-weighted MRI. *Magnetic Resonance in Medicine, 19*, 321–326.

Mukherjee, P., Miller, J. H., Shimony, J. S., Conturo, T. E., Lee, B. C., Almli, C. R., et al. (2001). Normal brain maturation during childhood: developmental trends characterized with diffusion-tensor MR imaging. *Radiology, 221*, 349–358.

Papadakis, N. G., Martin, K. M., Mustafa, M. H., Wilkinson, I. D., Griffiths, P. D., Huang, C.L., et al. (2002). Study of the effect of CSF suppression on white matter diffusion anisotropy mapping of healthy human brain. *Magnetic Resonance in Medicine, 48*, 394–398.

Parmar, H., Sitoh, Y. Y., & Yeo, T. T. (2004). Combined magnetic resonance tracotgraphy and functional magnetic resonance imaging in evaluation of brain tumors involving the motor system. *Journal of Computer Assisted Tomography, 28*, 551–556

Pajevic, S., & Pierpaoli, C. (1999). Color schemes to represent the orientation of anisotropic tissues from diffusion tensor data: application to white matter fiber tract mapping in the human brain. *Magnetic Resonance in Medicine, 42*, 526–540.

Pasternak, O., Sochen, N., & Assaf, Y. (2004). Separation of white matter fascicles from diffusion MRI using ϕ-functional regularization. *Proceedings of the International Society for Magnetic Resonance in Medicine, 12*, 1227.

Pasternak, O., Sochen, N., & Assaf, Y. (2006). PDE based estimation and regularization of multiple diffusion tensor fields. In J. Weickert & H. Hagen (Eds.), *Visualization and image processing of tensor fields.* Berlin: Springer.

Papadakis, N. G., Xing, D., Houston, G. C., Smith, J. M., Smith, M. I., James, M. F., et al. (1999). A study of rotationally invariant and symmetric indices of diffusion anisotropy. *Magnetic Resonance Imaging, 17*, 881–892.

Pierpaoli, C., & Basser, P. J. (1996). Toward a quantitative assessment of diffusion anisotropy. *Magnetic Resonance in Medicine, 36*, 893–906.

Pierpaoli, C., Jezzard, P., Basser, P. J., Barnett, A., & Di Chiro, G. (1996). Diffusion tensor MR imaging of the human brain. *Radiology, 201*, 637–648.

Poupon, C., Clark, C. A., Frouin, V., Regis, J., Bloch, I., Le Bihan, D., et al. (2000). Regularization of diffusion-based direction maps for the tracking of brain white matter fascicles. *NeuroImage, 12*, 184–195.

Price, G., Bagary, M. S., Cercignani, M., Altmann, D. R., & Ron, M. A. (2005). The corpus callosum in first episode schizophrenia: a diffusion tensor imaging study. *Journal of Neurology, Neurosurgery and Psychiatry, 76*, 585–587.

Sakuma, H., Nomura, Y., Takeda, K., Tagami, T., Nakagawa, T., Tamagawa, Y., et al. (1991). Adult and neuonatal human brain: diffusional anisotropy and myelination with diffusion-weighted MR imaging. *Radiology, 180*, 229–233.

Salat, D. H., Tuch, D. S., Greve, D. N., van der Kouwe, A. J., Hevelone, N. D., Zaleta, A. K., et al. (2005). Age-related alterations in white matter microstructure measured by diffusion tensor imaging. *Neurobiology Aging, 26*, 1215–1227.

Schonberg, T., Pianka, P., Hendler, T., Pasternak, O., & Assaf, Y. (2005). Characterization of displaced white matter by brain tumor by fMRI and DTI. *NeuroImage, 30*, 1100–1111, 2006.

Sinha, S., Bastin, M. E., Whittle, I. R., & Wardlaw, J. M. (2002). Diffusion tensor MR imaging of high-grade cerebral gliomas. *American Journal of Neuroradiology, 23*, 520–527.

Sorensen, A. G., Wu, O., Copen, W. A., Davis, T. L., Gonzalez, R. G., Koroshetz, W. J., et al. (1999). Human acute cerebral ischemia: detection of changes in water diffusion anisotropy by using MR imaging. *Radiology, 212*, 785–792.

Sotak, C. H. (2002). The role of diffusion tensor imaging in the evaluation of ischemic brain injury—a review. *NMR in Biomedicine, 15*, 561–569.

Szeszko, P. R., Ardekani, B. A., Ashtari, M., Malhotra, A. K., Robinson, D. G., Bilder, R. M., et al. (2005). White matter abnormalities in obsessive-compulsive disorder: a diffusion tensor imaging study. *Archives of General Psychiatry, 67*, 782–790.

Thomalla, G., Glauche, V., Koch, M. A., Beaulieu, C., Weiller, C., & Rother, J. (2004). Diffusion tensor imaging detects early Wallerian degeneration of the pyramidal tract after ischemic stroke. *NeuroImage, 22*, 1767–1774.

Tuch, D. S. (2004). Q-ball imaging. *Magnetic Resonance in Medicine, 52*, 1358–1372.

Tuch, D. S., Reese, T. G., Wiegell, M. R., Makris, N., Belliveau, J. W., & Wedeen, V. J. (2002). High angular resolution diffusion imaging reveals intravoxel white matter fiber heterogeneity. *Magnetic Resonance in Medicine, 48*, 577–582.

Tuch, D. S., Reese, T. G., Wiegell, M. R., & Wedeen, V. J. (2003). Diffusion MRI of complex neural architecture. *Neuron, 40*, 885–895.

Ulug, A. M., & van Zijl, P. C. (1999). Orientation-independent diffusion imaging without tensor diagonalization: anisotropy definitions based on physical attributes of the diffusion ellipsoid. *Journal of Magnetic Resonance Imaging, 9*, 804–813.

Werring, D. J., Clark, C. A., Barker, G. J., Thompson, A. J., & Miller, D. H. (1999). Diffusion tensor imaging of lesions and normal-appearing white matter in multiple sclerosis. *Neurology, 52*, 1626–1632.

Werring, D. J., Toosy, A. T., Clark, C. A., Parker, G. J., Barker, G. J., Miller, D. H., et al. (2000). Diffusion tensor imaging can detect and quantify corticospinal tract degeneration after stroke. *Journal of Neurology, Neurosurgery and Psychiatry, 69*, 269–272.

Westin, C. F., Maier, S. E., Mamata, H., Nabavi, A., Jolesz, F. A., & Kikinis, R. (2002). Processing and visualization for diffusion tensor MRI. *Medical Image Analysis, 6*, 93–108.

Wick, W., & Kuker, W. (2004). Brain edema in neurooncology: radiological assessment and management. *Onkologie, 27*, 261–266.

Witwer, B. P., Moftakhar, R., Hasan, K. M., Deshmukh, P., Haughton, V., Field, A., et al. (2002). Diffusion tensor imaging of white matter tracts in patients with cerebral neoplasm. *Journal of Neurosurgery, 97*, 568–575.

Yang, Q., Tress, B. M., Barber, P. A., Desmond, P. M., Darby, D. G., Gerraty, R. P., et al. (1999). Serial study of apparent diffusion coefficient and anisotropy in patients with acute stroke. *Stroke, 30*, 2382–2390.

Zelaya, F., Flood, N., Chalk, J. B., Wang, D., Doddrell, D. M., Strugnell, W., et al. (1999). An evaluation of the time dependence of the anisotropy of the water diffusion tensor in acute human ischemia. *Magnetic Resonance Imaging, 17*, 331–348.